21st Australasian Fluid Mechanics Conference
Adelaide, Australia
10-13 December 2018

Quadrant Analysis of Couette-Poiseuille Flows on the Verge of Separation

Zehuan Wu[1], Atsushi Sekimoto[1,2], Callum Atkinson[1] and Julio Soria[1]

[1]Laboratory for Turbulence Research in Aerospace and Combustion
Department of Mechanical and Aerospace Engineering, Monash University, Victoria 3800, Australia

[2]Department of Materials Engineering Science
Osaka University, Osaka 560-8531, Japan

Abstract

A numerical experiment using direct numerical simulation (DNS) of the particular Couette-Poiseuille (C-P) flow in which the pressure gradient dP/dx is adjusted to create zero mean skin friction on the stationary wall is conducted. The quadrant analysis of the Reynolds stress is performed based on data from the DNS with emphasis on the structures near the frictionless wall. Reynolds structures are motions of the Reynolds stress $u'v'$ and their structure is investigated by quadrant analysis which splits the values of Reynolds stress into four quadrants (Qs). A fully resolved case with Reynolds number equal to 2880 is used. The Reynolds number Re is defined using the velocity of the moving wall u_{wall}, viscosity ν and the half channel height h. Statistical and geometric characters of the Qs structures are investigated and reported.

Introduction

We are interested in coherent structures of wall-bounded turbulent flows in adverse pressure gradient (APG) environment because they have significant importance in drag reduction and separation control. The C-P flows are chosen to be studied as the fully developed flow is independent of initial condition and homogenous in streamwise and spanwise directions by its definition. C-P flow is the wall-bounded flows with a moving wall and a stationary wall subjected to a pressure gradient. In the first stage of our work[11], we investigated the effect of the size of the computational domain on large-scale structures by examining the pre-multiplied energy spectra and length scales of large-scale structures using data from DNS of C-P flows with different computational domains. The object of present work is to study coherent structures of the instantaneous Reynolds stress.

The Reynolds stress is the reason of 'sweeps' and 'ejections' which are related to the burst phenomenon that creates most of turbulent productions[4]. Several conditional sampling techniques have been developed to study Reynolds stress structures such as the VITA (variable interval time average)[2] and the VISA (variable interval space average)[5] and have been evaluated by Bogard *et al*. [3]. Base on the conclusion made by Bogard, the quadrant analysis provides the best balance between the probability of detection and false position.

In the quadrant analysis, the Reynolds stress is classified into four quadrants based on the values of streamwise and wall-normal velocity fluctuations (u' and v'). Quadrants are defined in the same way by Wallace *et al*.[10] as: Q1 events with $u' > 0$ and $v' > 0$, Q2 events (ejections) which have $u' < 0$ and $v' > 0$, Q3 events with $u' < 0$ and $v' < 0$ and Q4 events (sweeps) with $u' > 0$ and $v' < 0$. All Q events will be mentioned as Qs, Q2 and Q4 will be mentioned as Q^-.

Numerical Method and Structure Identification Method

In the simulation, the Navier-Stokes equations for incompressible flow are solved in the form of evolution equations for the wall-normal vorticity and the Laplacian of the wall-normal velocity[6]. The spectra method is used for spatial differentiation and discretization including Fourier expansion with 2/3 dealiasing applied in streamwise and spanwise directions and Chebychev polynomial in the wall-normal direction. The time advancement scheme is the three-step Runge-Kutta scheme. The detailed algorithm in the DNS is reported in [9, 8]. By using this method, a case with $Re = 2880$ is simulated and the parameters are summarized in table 1.

Following Lozano-Durán et al.[7], Reynolds structures are defined as region satisfying

$$\frac{|u'(x,y,z)v'(x,y,z)|}{u_{rms}(y)v_{rms}(y)} > H, \tag{1}$$

where u_{rms} and v_{rms} are the root mean square velocity fluctuations in streamwise and spanwise directions and H is the hyperbolic-hole size. The quadrant analysis highly depends on the value of H which is decided by a percolation analysis. A proper value of H should be chosen at where the number of Qs reaches its maximum and the ratio of the volume of the largest structures and total detected structures is located in a reasonable range. This means the largest structure is broken into separate structures and the value of H is high enough. Each structure is identified as a valid structure if the adjacent cells in the data set can be grouped as a continuous region satisfying 1. In addition, structures cross boundaries of the domain are rejected.

In our study, since we are interested in flow structures in the region near the frictionless wall, we also reject the structures whose the distance from the highest point to the moving wall ($2h - y_{max}$) is smaller than the distance from the lowest point to the stationary wall (y_{min}). This means we only take the structures which are closer to the stationary (frictionless) wall than to the moving wall into consideration and 166 statistically independent snapshots are used to study the structures.

Characterisation of Reynolds Structures

The result of the percolation analysis of identified Qs is shown in figure 1. It shows the percolation behaviour with the change of the hyperbolic-hole size H. When $H < 0.9$, the number of objects increases and $V_{largest}/V_{total}$ remains roughly constant which means the largest structure remains the same while other structures break into smaller structures. With H continuously increases, N_{max} drops rapidly and there is a sudden drop in $V_{largest}/V_{total}$, which implies the largest structure starts to break into separate structures and other structures start to be excluded due to the high value of H. The threshold used in present work is $H = 0.9$ where N_{max} reaches it maximum and the largest structure starts to break. It is noticed that this percolation behaviour is quite different compared with that of turbulent boundary layers [1] and turbulent channels [7], because the values of H at the turning points of $V_{largest}/V_{total}$ and $N_{objects}/N_{max}$ usually have

Case	Re	L_x	L_y	L_z	N_x	N_y	N_z	Δx^+	Δz^+	y_{10}^+	β
L2880	2880	$8\pi h$	$2h$	$4\pi h$	1280	257	1024	5.3	3.3	2.0	-672

Table 1: Parameters of the simulation. L_x, L_y and L_z are sizes of the domain in streamwise, wall-normal and spanwise directions. N_x, N_y and N_z are numbers of grid points in each direction. Δx^+ and Δz^+ are the grid spacing in viscous length scale defined in terms of the friction velocity u_τ at the moving wall and the kinematic viscosity ν. y_{10}^+ is the distance of the 10th gird from the wall in viscous length scale. β represents non-dimensional pressure gradient, $\beta = hP/\tau$, where P is the pressure gradient and τ is the wal shear stress at the stationary wall.

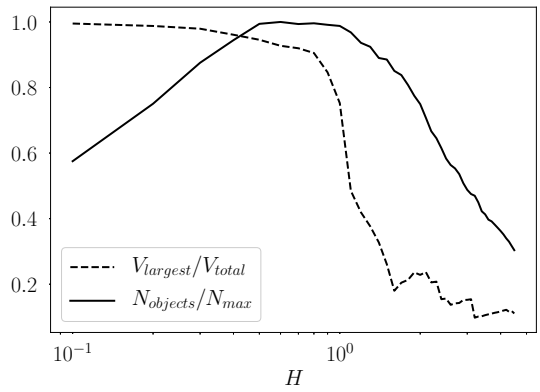

Figure 1: Percolation analysis for the identification of Qs. The blue line is the ratio of the volume of the largest structure ($V_{largest}$) to the volume of all Qs (V_{total}). The yellow line is the ratio of the number of identified Qs ($N_{objects}$) to the maximum number of Qs over H (N_{max}).

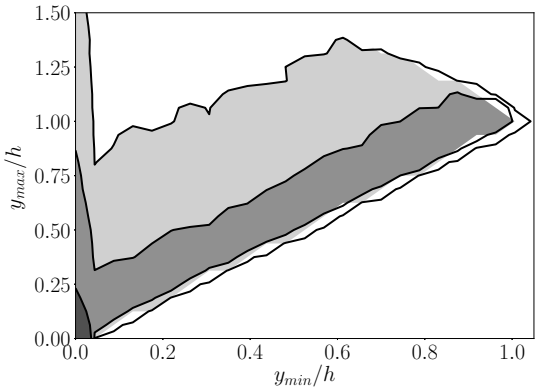

Figure 2: Joint probability density function of the maximum and minimum wall distances of Q^- structures, $p(y_{min}, y_{max})$. Contour levels are shown for 10, 1 and 0.1 from darker to lighter.

a big gap so that the balance between the volume and number of structures are hard to achieve.

The number of structures in each quadrant with respect to the total number of structures and the fraction of the volume of structures in each quadrant with respect to the total volume of the total channel volume are presented in table 2. It turns out that the number of Q^- structures takes only 34% of total Qs. The number of Q^- structures is reduced by APG, but the percentage of its volume is higher, so Q^- structures are not numerous but larger in volume than Q^+ structures. Q^- structures are the dominant structures rather than Q^+ structures near the stationary wall.

The geometric prosperities of Reynolds structures can be examined by the joint probability density function (p.d.f). Figure 2 shows the joint p.d.f of the minimum and maximum wall distances of Q^- structures. It shows that most structures evenly distributed from the stationary wall up to channel center. Some structures form near the stationary wall and cross deeply into the opposite half of the channel occupying about $3/4$ of the channel. Those very large structures are hard to see in the figure as the number of them is small, but their length-scale is large.

Figure 3 shows joint p.d.f.s of sizes of Q^- structures in streamwise l_x, spanwise l_z and wall-normal l_y directions. From figure 3(a), we can see that the shapes of the most of Q^- structures are long in streamwise direction but short in wall-normal direction. It seems APG restrains the sizes of Q^- structures in streamwise direction but extends the sizes of them in wall-normal direction. In figure 3(b), the dark area is less concentrated than that in figure 3(a). This indicates that there is no strong correlation between l_z and l_y. Figure 3(c) shows the distribution of the aspect ratio of Q^- structures. Despite some structures have l_z up to 10 times of l_y, the ratios of the spanwise size to the wall-normal size of the most of structures are distributed around 0.5 while the ratios of the streamwise size and the wall-normal size are around 1. This agrees with that those structures have larger streamwise size than the spanwise size. The distribution in figure 3(d) is roughly as same as figure 3(b). The average length of Q^- structures in streamwise $\langle l_x \rangle$, wall-normal $\langle l_y \rangle$ and spanwise $\langle l_z \rangle$ directions and the average minimum and maximum distance of Q^- structures from the frictionless wall ($\langle y_{min} \rangle$ and $\langle y_{min} \rangle$) are shown in table 3. On average, the streamwise sizes of the structures are about 2 times larger than their wall-normal sizes and the spanwise sizes are a bit larger than the wall-normal sizes.

Conclusions

Instantaneous Reynolds stress structures have been studied via quadrant analysis in a C-P flow with APG adjusted to create zero mean wall shear stress using DNS. The structures are identified by setting a threshold H to the local Reynolds stress and the appropriate value of the threshold is discussed based on percolation theory. The statistics of Reynolds structures in each quadrant are examined. In the region above the frictionless wall, The ratio of the number of Q^- to the number of Q^+ is roughly $1:1.8$ but the ratio of their volumes is approximately $4:1$. The distribution and geometric properties of Q^- structures are depicted by joint p.d.f.s. Some structures can occupy about 75% of the total channel hight. APG restrains the sizes of Q^- structures in streamwise direction and extends the sizes of them in wall-normal direction. The mean size of Q^- structures in each direction and the aspect ratio is discussed.

Acknowledgements

The computational facilities supporting this project include the Australian NCI National Facility, Pawsey Supercomputing Centre and the Multi-modal Australian Sciences Imaging and Visu-

Case	N_1	N_2	N_3	N_4	V_1	V_2	V_3	V_4
L2880	0.32	0.17	0.34	0.17	0.019	0.084	0.013	0.084

Table 2: Number of structures in each quadrant with respect to the total number of structures (N_{1-4}) and the volume of structures in each quadrant with respect to the total channel volume (V_{1-4}).

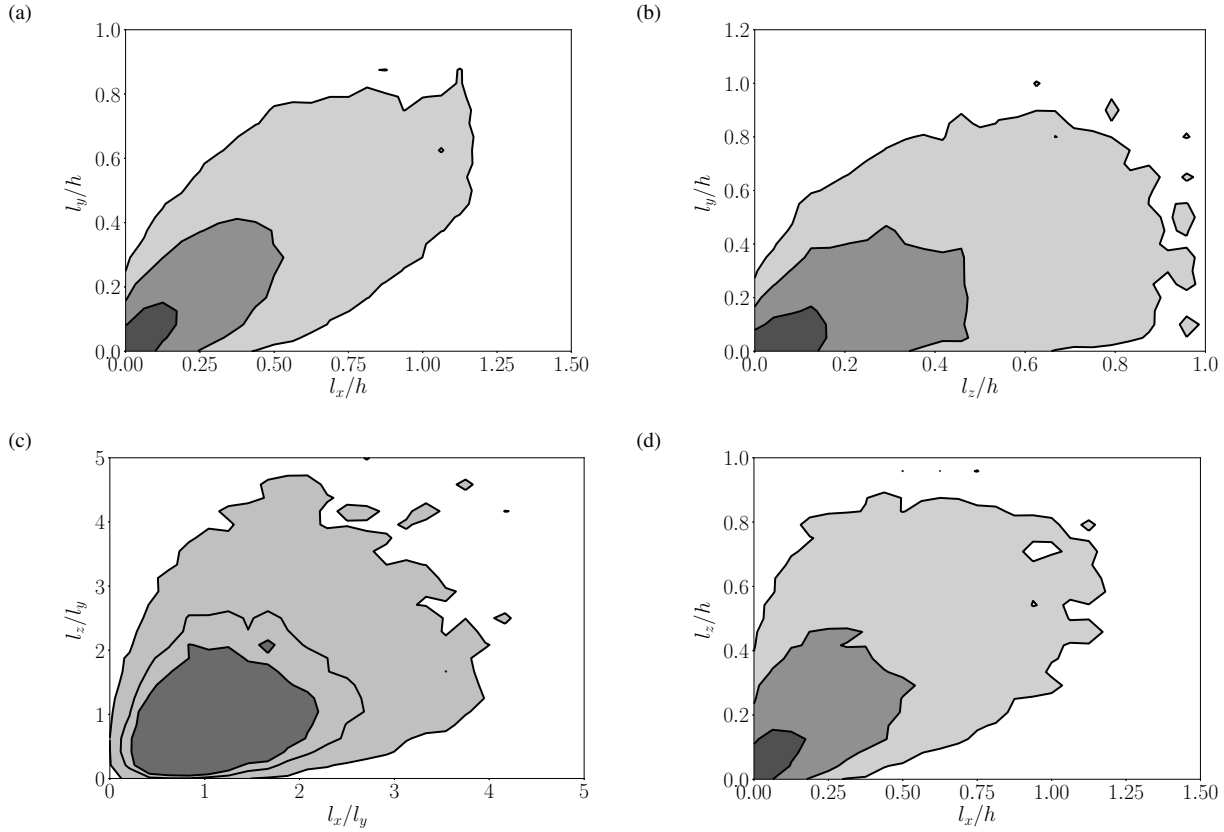

Figure 3: Joint p.d.f.s of sizes of Q^- structures in streamwise l_x, spanwise l_z and wall-normal l_y directions. (a) $p(l_x,l_y)$. (b) $p(l_z,l_y)$. (c) $p(l_x/l_y,l_z/l_y)$. (d) $p(l_x,l_z)$. Contour levels of (a), (b) and (d) are shown for 10, 1 and 0.1 from darker to lighter. Contour levels of (c) are shown for 0.1, 0.05 and 0.01.

$\langle l_x \rangle$	$\langle l_y \rangle$	$\langle l_z \rangle$	$\langle y_{min} \rangle$	$\langle y_{max} \rangle$
0.529	0.237	0.310	0.283	0.519

Table 3: Mean sizes of Q^- structures in streamwise $\langle l_x \rangle$, wall-normal $\langle l_y \rangle$ and spanwise $\langle l_z \rangle$ directions and the average minimum and maximum distance of Q^- structures from the frictionless wall ($\langle y_{min} \rangle$ and $\langle y_{max} \rangle$). All the values are scaled by the half channel hight h

alisation Environment (MASSIVE), which were provided by an NCMAS grant.

References

[1] Atkinson, C., Sekimoto, A., Jimnez, J. and Soria, J., Reynolds stress structures in a self-similar adverse pressure gradient turbulent boundary layer at the verge of separation, in *Journal of Physics: Conference Series*, **1001(1)**, 2018, 012001.

[2] Blackwelder, R.F. and Kaplan, R.E., On the wall structure of the turbulent boundary layer, *Journal of Fluid Mechanics*, **76(1)**, 1976, 89–112.

[3] Bogard, D.G. and Tiederman, W.G., Burst detection with single-point velocity measurements, *Journal of Fluid Mechanics*, **162**, 1986, 389–413.

[4] Kim, H., Kline, S.J. and Reynolds, W.C., The production of turbulence near a smooth wall in a turbulent boundary layer, *Journal of Fluid Mechanics*, **50(1)**, 1971, 133–160.

[5] Kim, J. and Moin, P., Application of a fractional-step method to incompressible navier-stokes equations, *Journal of computational physics*, **59(2)**, 1985, 308–323.

[6] Kim, J., Moin, P. and Moser, R., Turbulence statistics in fully developed channel flow at low reynolds number, *Journal of fluid mechanics*, **177**, 1987, 133–166.

[7] Lozano-Durán, A., Flores, O. and Jiménez, J., The three-dimensional structure of momentum transfer in turbulent channels, *Journal of Fluid Mechanics*, **694**, 2012, 100–130.

[8] Sekimoto, A., Atkinson, C. and Soria, J., Characterisation of minimal-span plane couette turbulence with pressure gradients, in *Journal of Physics: Conference Series*, **1001**, 2018, volume 1001, 012020.

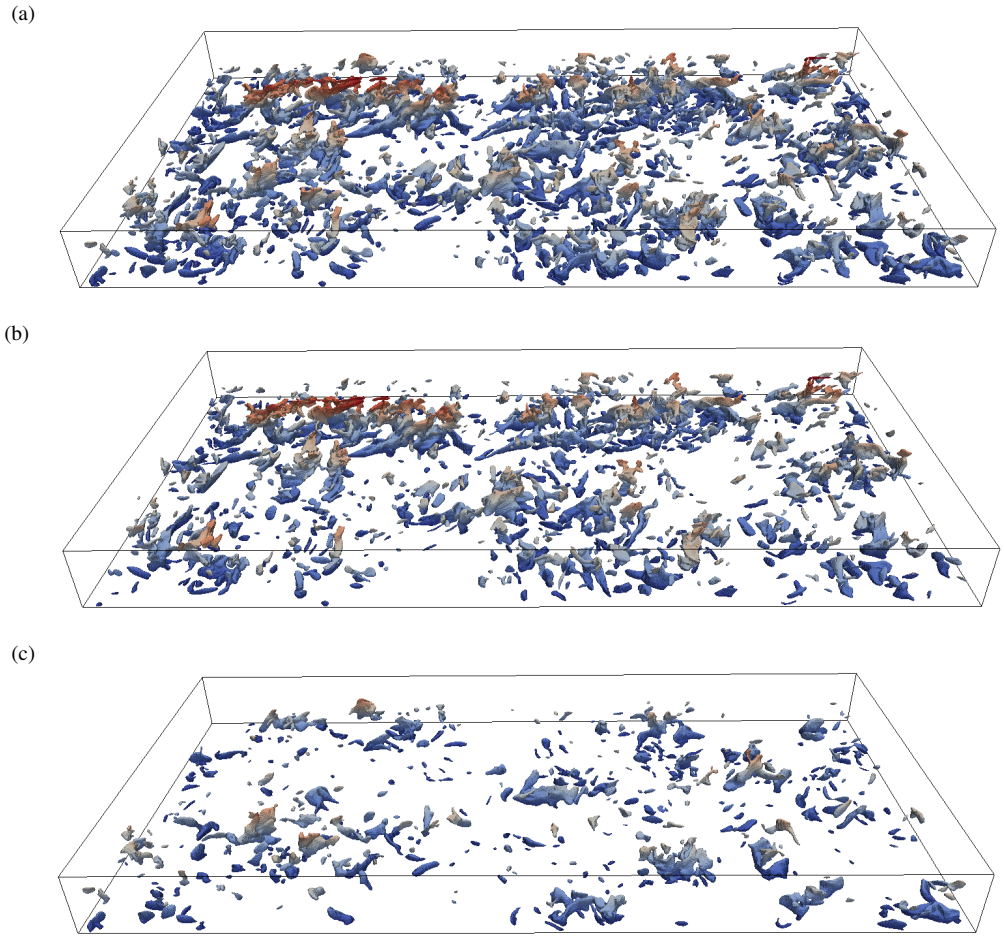

Figure 4: The instantaneous visualization of Qs structures including Q1-4 (a), Q^+ structures (b) and Q^- structures (c) coloured by the distance from the stationary wall (blue to red). The threshold of the isosurfaces is $H = 0.9$. The flow is from left to right.

[9] Sekimoto, A., Dong, S. and Jiménez, J., Direct numerical simulation of statistically stationary and homogeneous shear turbulence and its relation to other shear flows, *Physics of Fluids*, **28(3)**, 2016, 035101.

[10] Wallace, J.M., Eckelmann, H. and Brodkey, R.S., The wall region in turbulent shear flow, *Journal of Fluid Mechanics*, **54(1)**, 1972, 39–48.

[11] Wu, Z., Sekimoto, A., Atkinson, C. and Soria, J., Near-wall structures in couette-poiseuille flows on the verge of separation. in *Proceedings of the 11th Australasian Heat and Mass Transfer Conference*, 2018, 10.